Screening Currents and Hysteresis Losses in the REBCO Insert of the 32 T All-Superconducting Magnet Using *T-A* Homogenous Model

Edgar Berrospe-Juarez, Frederic Trillaud, Victor M. R. Zermeño, Francesco Grilli, Hubertus W. Weijers, and Mark D. Bird, *Senior Member, IEEE*

***Abstract*—The 32 T all-superconducting magnet of the National High Magnetic Field Laboratory (NHMFL) was successfully tested in December 2017 and it is expected to be soon available for users. This all-superconducting magnet, comprised of a high-temperature superconducting (HTS) insert and a low-temperature superconducting (LTS) outsert, is the first superconducting magnet reaching more than 30 T. One of the challenges facing this new magnet technology is the estimation of the screening currents, and the corresponding hysteresis losses in the two HTS coils. These coils are made of more than 20,000 turns of insulated REBCO conductor connected in series. The modelling of such system represents a significant challenge due to the huge computational load imposed by the size of the system. Up to now, only medium size magnets (made of units of thousands of turns/tapes) have been successfully modelled with methods based on the well-known *H* formulation of the Maxwell's equations. In the present work, a new model based on the *T-A* formulation and a homogeneous technique is proposed. This new approach greatly reduces the computational load and allows performing real-time simulations of large-scale HTS magnets on personal computers.**

***Index Terms*—Hysteresis losses, HTS magnets, REBCO tapes, large-scale superconductor systems, *T-A* formulation.**

Manuscript received September 22, 2019; accepted January 22, 2020. Date of publication January 28, 2020; date of current version February 19, 2020. This work was supported in part by the Programa de Maestría y Doctorado en Ingeniería of the Universidad National Autónoma de México (UNAM), in part by the Consejo Nacional de Ciencia y Tecnología (CONACYT) under Grant CVU: 490544, in part by the Dirección General de Asuntos del Personal Académico (DGAPA)–UNAM through PAPIIT-2017 under Grant #TA100617, in part by the PAPIIT-2019 under Grant #IN107119, in part by the National High Magnetic Field Laboratory supported by NSF cooperative Agreement DMR-1644779, and in part by the State of Florida. *(Corresponding authors: E. Berrospe-Juarez; V.M.R. Zermeño; F. Trillaud.)*

E. Berrospe-Juarez is with the Posgrado en Ingeniería Eléctrica, Universidad Nacional Autónoma de México, CDMX 04510, México (e-mail: eberrospej@iingen.unam.mx).

F. Trillaud is with the Instituto de Ingeniería, Universidad Nacional Autónoma de México, CDMX 04510, México (e-mail: ftrillaudp@iingen.unam.mx).

V. M. R. Zermeño is with the NKT, D-51061 Köln, Germany (e-mail: victor.zermeno@nkt.com).

F. Grilli is with the Institute for Technical Physics, Karlsruhe Institute of Technology, 76344 Eggenstein-Leopoldshafen, Germany (e-mail: francesco.grilli@kit.edu).

H. W. Weijers and M. D. Bird are with the National High Magnetic Field Laboratory, Tallahasee, FL 32310 USA.

Color versions of one or more of the figures in this article are available online at https://ieeexplore.ieee.org.

Digital Object Identifier 10.1109/TASC.2020.2969865

I. Introduction

HIGH magnet field facilities are built and operated to enable research in materials science. Nuclear fusion, medicine and pharmacology are among the areas of science that benefit from high magnetic field facilities [1]. The capacity of HTS material to maintain high critical currents under high magnetic fields has strongly stimulated the research towards a new generation of high-field magnets employing commercial HTS tapes [2]–[4]. The highest reported direct-current magnetic field is 45.5 T. This value was recently reached by a 14.4 T HTS test coil operated inside a 31.1 T resistive magnet [5]. This insert, called Little Big Coil (LBC), is part of the efforts undertaken at the NHMFL in Tallahassee, USA, to pave the way for the use of REBCO tapes in high-field magnets. The field generated by the LBC slightly exceeded the 45 T routinely provided to users in the NHMFL by a resistive-superconducting hybrid magnet that has been operational since 2000 [6]. There are many HTS inserts, test coils and user magnet projects around the world [7]–[15]. Within these projects, the all-superconducting (all-sc) magnet with the most intense field is the 32 T all-sc from the NHMFL [14], [15].

The electromagnetic modeling of the 32 T all-sc magnet is addressed in this paper. This magnet consists of a 17 T HTS insert and a 15 T LTS outsert. The HTS insert is made of REBCO tapes manufactured by SuperPower, Inc. In order to handle the extreme Lorentz's forces, the mechanical strength of the winding is increased by co-wounding the tapes with sol-gel plated stainless steel strips. The LTS outsert was custom-made by Oxford Instruments, Inc. The safe and reliable operation of the magnet is an important task that require the accurate estimation of the electromagnetic quantities. The computation of the hysteresis losses allows estimating the helium consumption and sizing the cryogenic system. The estimation of the current density distribution allows computing the magnetic field at the center of the magnet including the attenuation effect produced by the screening currents [16]–[18]. Even though not addressed in this paper, the correct estimation of the hoop stress also requires the knowledge of the current density distribution [19]. This information is also useful to improve the design of future high field magnets.

The well-known *H* formulation FEM models [20], [21] have been widely used during recent years to address the electromagnetic modeling of systems made of HTS tapes [22]. The main limitation for the analysis of large magnets, like the 32 T all-sc magnet, using this formulation is the huge amount of computational resources required to deal with a number of

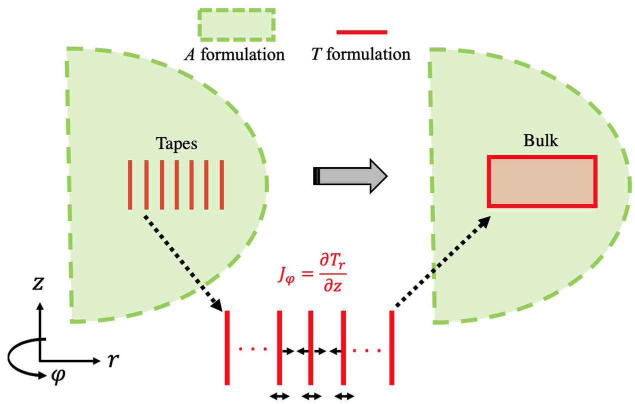

Fig. 1. The *T-A* formulation considers that superconducting layers are 1D objects. The homogenization process expands the thickness of the tapes absorbing the materials between the REBCO films to form a homogenous bulk.

degrees of freedom (DOF), on the order of the tens of millions. Three attempts have been made to deal with the electromagnetic modeling of the 32 T all-sc magnet. The study of smaller size prototype magnets was addressed using a homogeneous model in [23]. The model of the inner coil of the HTS insert, also using homogenous model, was presented in [19]. The multi-scale model of the full-sized HTS insert was presented in [24]. The homogenization and multi-scale methods, as described respectively in [25], [26], are used in conjunction with the *H* formulation and allow simplifying the system's description and build more efficient models with reduced numbers of DOF. Additionally, the analysis of the quench in the 32 T all-sc magnet has been carried out in [27]–[29].

In this paper we present the *T-A* homogenous model of the 32 T all-sc magnet. The *T-A* homogenous strategy was recently proposed in [30], and is based on the *T-A* formulation and the homogenization method. The *T-A* formulation was also recently proposed in [31], [32]. The *T-A* homogeneous strategy allows building more efficient models than those using the *H* formulation. Also, and more importantly, the *T-A* homogeneous model enables addressing the analysis of the full-sized HTS insert, considering the effect of the field generated by the LTS outsert, under the conditions imposed by a real charge cycle. Such analysis cannot be performed with the previously reported *H* formulation-based strategies.

II. *T-A* Homogenous Strategy

As suggested by its name, the *T-A* formulation is implemented by the combination of the *T* and the *A* formulations. In the *T-A* formulation the superconducting layer of the REBCO tapes are modelled as one dimensional (1D) objects. The medium that surrounds the superconducting layers is considered non-conductive. This medium represents not only the cryogenic liquid but also the metallic layers of the REBCO tapes. The current vector potential $\mathbf{T}$ is exclusively defined along the superconducting lines, and is given by $\mathbf{J} = \nabla \times \mathbf{T}$ [20]. In contrast, the magnetic vector potential $\mathbf{A}$ is defined over the entire geometry, and is given by $\mathbf{B} = \nabla \times \mathbf{A}$ [20].

Fig. 1 shows the 2D representation of an axisymmetric pancake. In a 2D geometry the only component of $\mathbf{A}$ is A_φ. In the 1D superconducting layers $\mathbf{J}$ is defined by $J_\varphi = \partial T_r/\partial z$. Then, the governing equations of the *A* and *T* formulations, respectively, are

$$\nabla^2 A_\varphi = -\mu_0 J_\varphi \tag{1}$$

$$\frac{\partial}{\partial z}\left(\rho_{HTS}\frac{\partial T_r}{\partial z}\right) = \frac{\partial B_r}{\partial t} \tag{2}$$

where μ_0 is the magnetic permeability of the vacuum, and ρ_{HTS} is the resistivity of the superconducting material. A detailed description of the *T-A* formulation can be consulted in [31], [32].

As depicted in Fig. 1, the homogenization process consists in transforming the composite pancakes into homogeneous bulks. Therefore, the gaps between adjacent superconducting layers disappear as the superconducting layers are expanded until a unique bulk is formed. Now, $\mathbf{T}$ is only defined inside the bulks and its computation does not take into account the influence of B_z (the component parallel to the surface of the tapes). Therefore, $\mathbf{T}$ has only one component defined by (2). A detailed description of the *T-A* homogenous strategy can be consulted in [30]. For the specific case of axisymmetric coils, an additional simplification of the model can be achieved by taking notice of the system's symmetries and reducing the solving region. Here only the right upper quadrant of the HTS insert is modeled.

The hysteresis losses are computed along the lines passing through the middle of each individual bulk's subsection. The losses in the rest of the tapes of each pancake are found by cubic spline interpolation. Finally, the total losses are computed by summing the losses in all the tapes. The PDE and AC/DC modules of the commercial software COMSOL Multiphysics 5.4 are used to implement the *T-A* homogenous model.

III. Magnet Description

The 32 T all-superconducting magnet consists of a 17 T HTS insert and a 15 T LTS outsert. The HTS insert comprises two concentric coils, here named Coil 1 and Coil 2. These coils consist of 20 and 36 double pancakes co-wound with insulated stainless steel and REBCO tapes. The REBCO tapes have a width of 4 mm and a thickness of approximately 170 μm, while the REBCO layer is 1 μm thick.

The LTS outsert, made of three Nb_3Sn coils and two NbTi coils, is modelled as 5 concentric coils in which a uniform current density is impressed to provide the expected magnetic flux density of 15 T at peak-field operation. This uniform current density is assumed to be independent of the field produced by the HTS insert. Table I outlines the most important parameters of the HTS insert and the LTS outsert. More details about the construction of the 32 T all-sc magnet can be found in [14], [15]. Fig. 2 shows the axisymmetric sketch of the magnet.

A. *Critical Current Density*

The resistivity of the superconducting material is modeled by the well-known power law

$$\rho_{HTS} = \frac{E_c}{J_c(\boldsymbol{B})}\left|\frac{\mathbf{J}}{J_c(\boldsymbol{B})}\right|^{n-1} \tag{3}$$

where $\mathbf{J}$ is the current density and J_c is the critical current density, both in A/m^2. The voltage criterion is chosen as $E_c = 1$ V/cm. The *n*-value is considered constant in the present work, $n = 25$.

TABLE I
32 T ALL-SUPERCONDUCTOR MAGNET'S PARAMETERS

HTS Insert		
Parameter	Coil 1	Coil 2
Inner rad. [mm]	20	82
Outer rad. [mm]	70	116
Height [mm]	178	320.4
Pancakes	40	72
Turns/Pancake	253	145

LTS Outsert					
Parameter	Coil 1	Coil 2	Coil 3	Coil 4	Coil 5
Inner rad. [mm]	134.93	171.81	213.89	256.77	288.55
Outer rad. [mm]	154.92	191.30	234.08	279.56	311.41
Height [mm]	517.40	557.20	597.00	636.80	636.80
Turns	5234	6662	8356	5302	7127

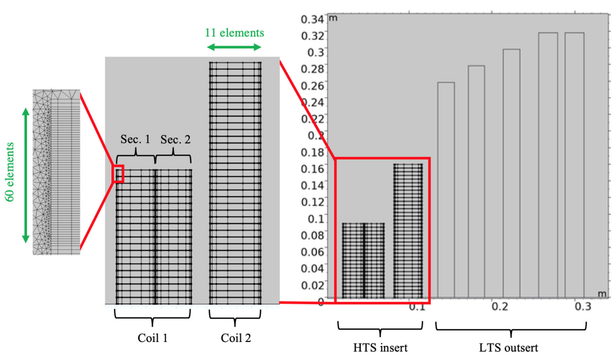

Fig. 2. Sketch of the 32 T all-sc magnet. The figure shows the HTS insert and the LTS outsert, the coils of the insert, as well as the sections of Coil 1. The mesh of the bulks considers 60 elements along the tape's width, and 11 elements along the coil/section's thickness.

The critical current density has anisotropic properties, its performances is affected by both the magnitude and direction of the magnetic field. The characterization of the HTS tape was carried out at NHMFL, by collecting I_c measurements at 4.2 K. The J_c was derived from the I_c measurements using the parameter-free method proposed in [33]. For easier handling, the data obtained with the free-parameter method were fitted to the following Kim-like formula

$$J_c\left(B_r, B_z\right) = \frac{\beta \cdot J_{c0}}{\left(1 + \frac{\sqrt{k^2 B_z^2 + B_r^2}}{B_0}\right)^{\alpha}} \tag{4}$$

where B_r and B_z are the radial and axial components of the magnetic flux density, respectively. The best fit parameters are: $J_{c0} = 7.24 \cdot 10^{11}\,\text{A/m}^2$, $B_0 = 0.4674$ T, $k = 9.13 \cdot 10^{-3}$, $\alpha = 0.7518$. The measured I_c vary from batch to batch, and the dimensionless coefficient β describes this variation.

Each pancake of Coil 2 is wound with a single piece of REBCO tape having the same I_c value, and therefore the same β coefficient. In contrast, each pancake of Coil 1 is wound with two pieces of tape having different I_c values. In order to handle this variation, the Coil 1 pancakes are further subdivided into two sections. Section I, going from tape 1 to tape 131, and Section II, going from tape 132 to tape 253. The β coefficient was estimated experimentally at NHMFL, and takes values ranging from 0.63 for the pancakes in the middle plane to 1.5 for the pancakes in the upper and lower positions.

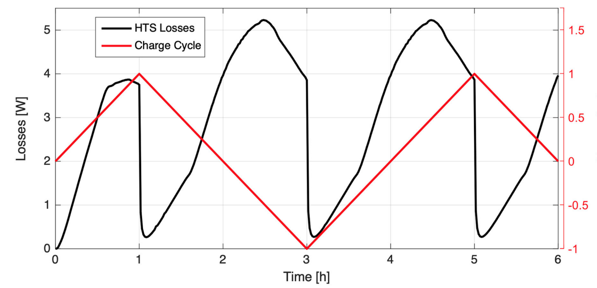

Fig. 3. The red line presents the normalized charge cycle. At the peak of the cycle, the magnetic flux density should be 32 T. The black line represents the instantaneous total hysteresis losses.

B. Homogeneous Bulks

The homogenous bulks representing the pancakes in the *T-A* homogenous model are meshed with rectangular elements considering 60 elements uniformly distributed along the tape's width. The mesh of the Coil 2 pancakes has 11 elements along the bulk's thickness. Previous results of this [24] and other coils [26] show that more significant variations in the losses are expected in the inner and outer tapes of the pancakes, then the elements' distribution considers an increasing number of elements at the bulk's extremities.

Because of the further division of the Coil 1 pancakes, each section considers a mesh with 11 elements along each section's thickness. The transition between sections with different coefficient β produces drastic variations in $\mathbf{J}$ and in the losses at the middle of Coil 1. In order to avoid this numerical artifact, it is considered that β experiences a linear change starting at tape 128 and finishing at tape 134.

IV. SIMULATION AND DISCUSSION

The charge cycle, simulated in this paper, represents a real operating condition for the magnet. The currents in the HTS insert and the LTS outsert have the triangular shape presented with red line in Fig. 3. The current amplitudes are 173 A and 268 A in the insert and outsert, respectively. The simulated time-lapse sums up to 6 h.

The magnet flux density magnitude in the insert and the outsert, as well as the normalized current density ($J_n = \mathbf{J}/J_c$) in the insert, at the first peak of the charge cycle ($t = 1$ h) are shown in Fig. 4. The screening currents are induced by the penetration of the magnetic field into the tapes. At these field values, the screening currents are such that the upper pancakes, especially those of Coil 2, are fully penetrated mainly by these screening currents.

A. Losses

The instantaneous power dissipation as a function of time during the simulated lapse is presented with a black line in Fig. 3. The total hysteresis losses summed up during the 6 h charge cycle are Q = 61.08 kJ. The losses in the first third of the charge cycle are lower than the losses in the subsequent two thirds. 29% of the losses occur during this first third of the cycle. The losses

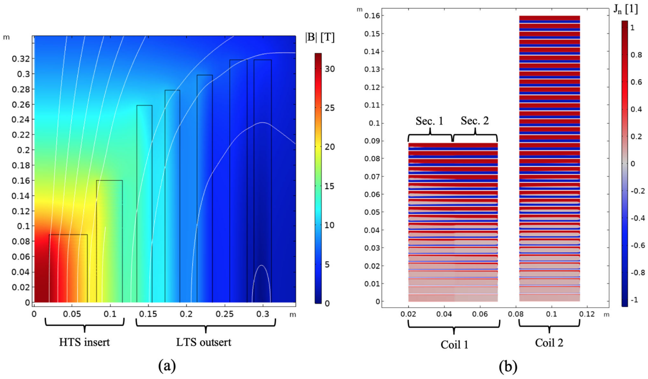

Fig. 4. (a) Magnetic flux density magnitude and (b) normalized current density at 1 h, the first peak of the ramping cycle. The upper pancakes are fully penetrated by screening currents.

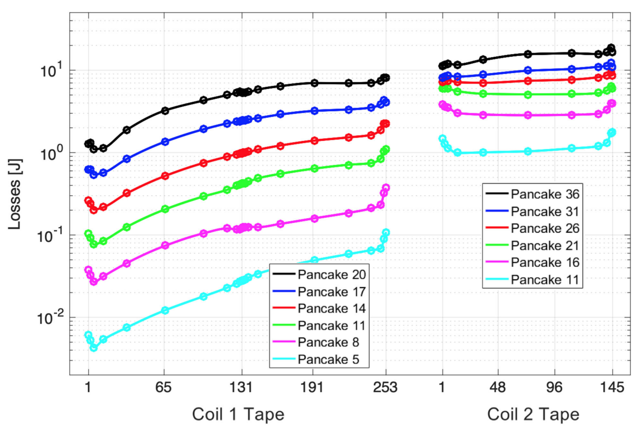

Fig. 5. Losses in selected pancakes of both coils of the HTS insert during all the simulated time-lapse.

after the first third are periodic, as well as the charge cycle, this means that the transient behavior occurs in the first third of the charge cycle.

The losses in some representative pancakes as a function of the tape's number are shown in Fig. 5. In this plot the x-axis represents the tape's number inside the pancakes. It can be noted that the pancakes at the upper positions have higher losses; this behavior has been previously observed in [25], [26]. This behavior results from the impact of the highest horizontal component of the magnetic field on the J_c in the upper pancakes. As expected from Fig 5, the losses are greater in Coil 2 than in Coil 1 with 83% of the total losses taking place in the former.

B. Screening Current-Induced Field

A direct consequence of the screening currents is the attenuation of the central magnetic flux density, referred to as screening current-induced field (SCIF) [34] which is usually defined as

$$B_{SCIF} = B_{\rm sim} - B_n \tag{5}$$

where $B_{\rm sim}$ is the field computed at the center of the screening currents. The nominal field B_n is the field considering uniform current distributions flowing in both the insert and the outsert. The SCIF versus B_n exhibits hysteresis. The simulated lapse is enough to retrieve the full hysteresis loop shown in Fig. 6. $B_{\rm sim}$ at the peak of the charge cycle is 31.09 T, which is almost 1 T

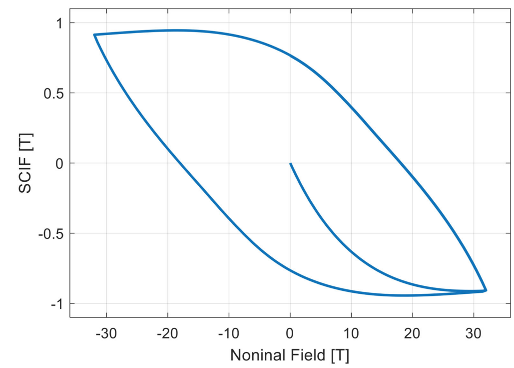

Fig. 6. SCIF (B_{SCIF}) versus nominal field (B_n), the lapse of the charge cycle allows to retrieve the hysteresis loop.

lower than the expected 32 T, while the remnant field at 0 A is 0.77 T.

The proposed model is intended to be a guide for future experiments and for the establishment of safe operation limits for the magnet. The comparison of the estimated losses against experimental data is hindered by the difficulty of distinguishing the hysteresis losses contribution from all the losses. The J_c strongly affects the shape of the SCIF loop [17], and the mechanical stress degrades J_c [35], [36]. For a fair comparison of the SCIF, the numerical model should couple the mechanic and electromagnetic phenomena. Such comparisons against experimental results are beyond the scope of the manuscript. It is worth mentioning that the *T-A* homogenous strategy has been validated against the *H* formulation strategy [30], and this latter has been validated against experimental data [37], [38].

The computer used to conduct the simulations is a desktop computer (6 cores, Intel (R) Xeon(R) ES-2630, 2.2 GHz, 64 GB RAM). The time required to simulate the 6 h cycle with the *T-A* homogenous model is 5 h 29 min. This computation time is a clear demonstration of the *T-A* homogenous model is more efficient than the iterative multi-scale model. For instance, it is reported in [24], that the computation time required to run a simulation with the iterative multi-scale model is around 19 days. It should be stressed that the simulation reported in [24] does not consider the effect of the LTS outsert, and the charge cycle does not represent a real-case scenario.

V. Conclusion

The electromagnetic quantities in the HTS insert of the 32 T all-superconducting magnet were successfully estimated using a *T-A* homogenous model. This model allows estimating the current density distribution inside the pancakes' tapes, therefore enabling the estimation of the hysteresis losses as well as the SCIF. The knowledge of such quantities is important to provide information to optimize the cooling system, estimate the cost of operating the facility as well as establishing safe operational margins for the magnet.

When compared with other models, i.e., *H* homogeneous and multi-scale, the *T-A* homogeneous model significantly reduces the computational load making possible the following characteristics: (i) It is possible to model the full-size HTS insert. (ii) It is possible to include the background magnetic field produce by the LTS outsert. (iii) It is possible to perform real-time simulations for charge cycles with periods in the order of the hours using an ordinary desktop computer.

References

[1] *High Magnetic Field Science and its Application in the United States: Current Status and Future Directions*, Washington, DC, USA: The National Academies Press, 2013.

[2] D. Abraimov *et al.*, "Double disordered YBCO coated conductors of industrial scale: High currents in high magnetic field," *Supercond. Sci. Technol.*, vol. 28, no. 11, 2015.

[3] K. Tsuchiya *et al.*, "Critical current measurement of commercial REBCO conductors at 4.2 K," *Cryogenics*, vol. 85, pp. 1–7, 2017.

[4] T. Benkel *et al.*, "Preliminary tests and margin estimate for a REBCO insulated 10 T insert under high magnetic field," *IEEE Trans. Appl. Supercond.*, vol. 27, no. 4, Jun. 2017, Art. no. 4602105.

[5] S. Hahn *et al.*, "45.5-tesla direct-current magnetic field generated with a high-temperature superconducting magnet," *Nature*, vol. 570, 2019, Art. no. 7762.

[6] J. R. Miller, "The NHMFL 45-T hybrid magnet system: Past, present, and future," in *IEEE Trans. Appl. Supercond.*, vol. 13, no. 2, pp. 1385–1390, Jun. 2003.

[7] H. Maeda and Y. Yanagisawa, "Recent developments in high-temperature superconducting magnet technology (Review)," *IEEE Trans. Appl. Supercond.*, vol. 24, no. 3, Jun. 2014, Art. no. 4602412.

[8] J. Liu, L. Wang, L. Qin, Q. Wang, and Y. Dai, "Recent development of the 25T all-superconducting magnet at IEE," *IEEE Trans. Appl. Supercond.*, vol. 28, no. 4, Jun. 2018, Art. no. 4301305.

[9] S. Yoon, J. Kim, H. Lee, S. Hahn, and S. H. Moon, "26 T 35 mm all-$GdBa_2$ Cu_3 $O_{7\text{-}x}$ multi-width no-insulation superconducting magnet," *Supercond. Sci. Technol.*, vol. 29, no. 4, 2016.

[10] H. Schwalbe, "Editorial: New 1.2 GHz NMR spectrometers—New horizons?" *Angew. Chemie - Int. Ed.*, vol. 56, no. 35, pp. 10252–10253, 2017.

[11] S. Awaji *et al.*, "First performance test of a 25 T cryogen-free superconducting magnet," *Supercond. Sci. Technol.*, vol. 30, no. 6, 2017, Art. no. 065001.

[12] H. Maeda, J. I. Shimoyama, Y. Yanagisawa, Y. Ishii, and M. Tomita, "The MIRAI program and the new super-high field NMR initiative and its relevance to the development of superconducting joints in Japan," *IEEE Trans. Appl. Supercond.*, vol. 29, no. 5, Aug. 2019, Art. no. 4602409.

[13] T. Benkel *et al.*, "REBCO performance at high field with low incident angle and preliminary tests for a 10-T insert," *IEEE Trans. Appl. Supercond.*, vol. 26, no. 3, Apr. 2016, Art. no. 4302705.

[14] W. D. Markiewicz *et al.*, "Design of a superconducting 32 T magnet with REBCO high field coils," *IEEE Trans. Appl. Supercond.*, vol. 22, no. 3, Jun. 2012, Art. no. 4300704.

[15] H. W. Weijers *et al.*, "Progress in the development and construction of a 32-T superconducting magnet," *IEEE Trans. Appl. Supercond.*, vol. 26, no. 4, Jun. 2016, Art. no. 4300807.

[16] Y. Yanagisawa *et al.*, "Effect of YBCO-coil shape on the screening current-induced magnetic field intensity," *IEEE Trans. Appl. Supercond.*, vol. 20, no. 3, pp. 744–747, Jun. 2010.

[17] Y. Yanagisawa *et al.*, "Magnitude of the screening field for YBCO coils," *IEEE Trans. Appl. Supercond.*, vol. 21, no. 3, pp. 1640–1643, Jun. 2011.

[18] Y. Li *et al.*, "Magnetization and screening current in an 800-MHz (18.8-T) REBCO NMR insert magnet: Experimental results and numerical analysis," *Supercond. Sci. Technol.*, 32, no. 10, 2019.

[19] J. Xia, H. Bai, H. Yong, H. W. Weijers, T. A. Painter, and M. D. Bird, "Stress and strain analysis of a REBCO high field coil based on the distribution of shielding current," *Supercond. Sci. Technol.*, vol. 32, no. 9, 2019.

[20] F. Grilli, R. Brambilla, F. Sirois, A. Stenvall, and S. Memiaghe, "Development of a three-dimensional finite-element model for high-temperature superconductors based on the H-formulation," in *Cryogenics*, vol. 53, pp. 142–147, 2013.

[21] Z. Hong, A. M. Campbell, and T. A. Coombs, "Numerical solution of critical state in superconductivity by finite element software," *Supercond. Sci. Technol.*, vol. 19, no. 12, 2006, Art. no. 1246.

[22] B. Shen, F. Grilli, and T. A. Coombs, "Review of the AC loss computation for HTS using H formulation," *Supercond. Sci. Technol.*, 2020.

[23] J. Xia, H. Bai, J. Lu, A. V. Gavrilin, Y. Zhou, and H. W. Weijers, "Electromagnetic modeling of REBCO high field coils by the H-formulation," *Supercond. Sci. Technol.*, vol. 28, no. 12, 2015.

[24] E. Berrospe-Juarez *et al.*, "Estimation of losses in the (RE)BCO two-coil insert of the NHMFL 32 T all-superconducting magnet," *IEEE Trans. Appl. Supercond.*, vol. 28, no. 3, Apr. 2018, Art. no. 4602005.

[25] V. M. R. Zermeno, A. B. Abrahamsen, N. Mijatovic, B. B. Jensen, and M. P. Sørensen, "Calculation of alternating current losses in stacks and coils made of second generation high temperature superconducting tapes for large scale applications," *J. Appl. Phys.*, vol. 114, no. 17, 2013.

[26] E. Berrospe-Juarez, V. M. R. Zermeño, F. Trillaud, and F. Grilli, "Iterative multi-scale method for estimation of hysteresis losses and current density in large-scale HTS systems," *Supercond. Sci. Technol.*, vol. 31, no. 9, 2018.

[27] M. Breschi, L. Cavallucci, P. L. Ribani, A. V. Gavrilin, and H. W. Weijers, "Modeling of quench in the coupled HTS insert/LTS outsert magnet system of the NHMFL," *IEEE Trans. Appl. Supercond.*, vol. 27, no. 5, Aug. 2017, Art. no. 4301013.

[28] L. Cavallucci, M. Breschi, P. L. Ribani, A. V. Gavrilin, H. W. Weijers, and P. D. Noyes, "A numerical study of quench in the NHMFL 32 T magnet," *IEEE Trans. Appl. Supercond.*, vol. 29, no. 5, Aug. 2019, Art. no. 4701605.

[29] M. Breschi, L. Cavallucci, P. L. Ribani, A. V. Gavrilin, and H. W. Weijers, "Analysis of quench in the NHMFL REBCO prototype coils for the 32 T magnet project," *Supercond. Sci. Technol.*, vol. 29, no. 5, 2016, Art. no. 055002.

[30] E. Berrospe-Juarez, V. M. R. Zermeño, F. Trillaud, and F. Grilli, "Real-time simulation of large-scale HTS systems: Multi-scale and homogeneous models using the T–A formulation," *Supercond. Sci. Technol.*, vol. 32, no. 6, 2019.

[31] H. Zhang, M. Zhang, and W. Yuan, "An efficient 3D finite element method model based on the T-A formulation for superconducting coated conductors," *Supercond. Sci. Technol.*, vol. 30, no. 2, 2017, Art. no. 024005.

[32] F. Liang *et al.*, "A finite element model for simulating second generation high temperature superconducting coils/stacks with large number of turns," *J. Appl. Phys.*, vol. 122, no. 4, 2017, Art. no. 043903.

[33] V. M. R. Zermeño, K. Habelok, M. Stępień, and F. Grilli, "A parameter-free method to extract the superconductor's J c(B,θ) field-dependence from in-field current-voltage characteristics of high temperature superconductor tapes," *Supercond. Sci. Technol.*, vol. 30, no. 3, 2017, Art. no. 034001.

[34] K. L. Kim *et al.*, "Study on elimination of screening-current-induced field in pancake-type non-insulated HTS coil," *Supercond. Sci. Technol.*, vol. 29, no. 3, 2016, Art. no. 035009.

[35] H. S. Shin, K. H. Kim, J. R. C. Dizon, T. Y. Kim, R. K. Ko, and S. S. Oh, "The strain effect on critical current in YBCO coated conductors with different stabilizing layers," in *Supercond. Sci. Technol.*, vol. 18, no. 12, 2005.

[36] G. Majkic, R. J. Mensah, V. Selvamanickam, Y. Y. Xie, and K. Salama, "Electromechanical behavior of IBAD/MOCVD YBCO coated conductors subjected to torsion and tension loading," in *IEEE Trans. Appl. Supercond.*, vol. 19, no. 3, pp. 3003–3008, Jun. 2009.

[37] G. G. Sotelo, M. Carrera, J. Lopez-Lopez, and X. Granados, "H-formulation FEM modeling of the current distribution in 2G HTS tapes and its experimental validation using hall probe mapping," *IEEE Trans. Appl. Supercond.*, vol. 26, no. 8, Dec. 2016, Art. no. 6603510.

[38] B. Shen *et al.*, "Investigation of AC losses in horizontally parallel HTS tapes," *Supercond. Sci. Technol.*, vol. 30, no. 7, 2017.